Surface Science 689 (2019) 121451

Contents lists available at ScienceDirect

Surface Science

journal homepage: www.elsevier.com/locate/susc

Selective resolution of phonon modes in STM-IETS on clean and oxygen-adsorbed Cu(100) surfaces

Lee Minjun[a], Oh Myungchul[a], Jeon Hoyeon[a], Yi Sunwouk[a], Zoh Inhae[a], Zhang Chao[a], Chae Jungseok[b,c,*], Kuk Young[a,d,**]

[a] Department of Physics and Astronomy, Seoul National University, Seoul 08826, Republic of Korea
[b] Center for Quantum Nanoscience, Institute for Basic Science, Seoul 03760, Republic of Korea
[c] Department of Physics, Ewha Womans University, Seoul 03760, Republic of Korea
[d] Department of Emerging Materials Science, Daegu-Gyeongbuk Institute of Science and Technology, Republic of Korea

A B S T R A C T

The observation of surface phonon using scanning probe microscopy can provide important information related to local structural and electrical properties. In this study, surface phonon modes on a Cu(100) surface were measured using inelastic tunneling spectroscopy of scanning tunneling microscopy. One phonon mode was measured at 3.6 meV on a clean Cu(100) surface. On an oxygen-adsorbed Cu(100) surface, another phonon mode was measured at 13.5 meV. This phonon mode was considered to be enhanced by the symmetry created by Cu-missing rows. The spatially varying d^2I/dV^2 map showed the effect of surface stress relaxation.

Surface phonon modes can differ from bulk phonon modes because they arise from the abrupt termination of a crystal structure at a surface. Surface phonon dispersion has been measured by electron energy loss spectroscopy (EELS) [1] and He atom scattering (HAS) [2]. However, these methods measure the averaged dispersions over the beam spot size, thereby limiting the spatial resolution [3]. To understand the local properties of surface phonon modes related to surface structures, a local probe method is required. Since vibration spectroscopy with a local probe was first realized using the inelastic tunneling spectroscopy (IETS) of scanning tunneling microscopy (STM) [4], it has become a powerful method to measure molecular vibrational modes in single molecules [5–7] and spin excitation in single magnetic atoms [8–11] on various surfaces. Molecular vibrations are localized within a single molecule; by contrast, surface phonons originate from the quantization of collective lattice vibrations over a surface. However, despite this difference, STM-IETS can be used to measure the excitation of surface phonon modes with the same measurement principle as that for molecular vibrations. On graphite and graphene surfaces, which have a covalent bonding nature, surface phonon modes were measured using STM-IETS [12,13] at theoretically predicted van Hove singularities (VHSs). On metal surfaces, however, the observed acoustic phonon peaks were broad [14,15], and the optical phonon peaks were hardly detected in STM-IETS measurements.

Although the mechanism of opening of an inelastic tunneling channel by a surface phonon is not yet clearly understood, it was suggested that a tunneling electron is coupled to a surface phonon [15]. Therefore, the measured inelastic tunneling signal is proportional to the product of the electron–phonon coupling matrix elements and the phonon density of states. Consequently, the momentum-averaged tunneling matrix limits the energy resolution of the phonon mode compared with the molecular vibration spectra in STM-IETS. In a recent study [16], It was found that the peak height of inelastic signal was determined by the atomic configuration of the probing tip in STM-IETS. A single-atom tip yields an enhanced STM-IETS signal on top of a CO molecule on the Cu(111) surface compared with three- or four-atom tip configurations. According to theoretical studies on STM-IETS [17,18], the STM-IETS signal is dependent on the relaxation energy of the atom under the tip, which opens the inelastic tunneling channels and can be affected by the presence of a sharp STM tip. Based on this experimental and theoretical background, we measured the surface phonon modes on a clean Cu(100) surface and oxygen-adsorbed Cu(100) surfaces by using atomically sharp STM tips prepared by field ion beam (FIB) sharpening followed by in situ annealing. Acoustic phonon modes were measured on Cu(100) and oxygen-adsorbed Cu(100) surfaces by using these tips. Moreover, a spatial variation map on oxygen-adsorbed surfaces shows locally enhanced d^2I/dV^2 signals, possibly due to local surface relaxation.

Before exploring oxygen-adsorbed surfaces, a clean Cu(100) surface was prepared by several cycles of Ar sputtering and annealing at 450 °C. Fig. 1(a) shows an STM topographic image of the clean Cu(100) surface,

* Corresponding author at: Center for Quantum Nanoscience, Institute for Basic Science, Seoul 03760, Republic of Korea.
** Corresponding author at: Department of Physics and Astronomy, Seoul National University, Seoul 08826, Republic of Korea.
E-mail addresses: chae.jungseok@qns.science (J. Chae), ykuk@phya.snu.ac.kr (Y. Kuk).

https://doi.org/10.1016/j.susc.2019.06.001
Received 31 March 2019; Received in revised form 27 May 2019; Accepted 1 June 2019
Available online 03 June 2019
0039-6028/

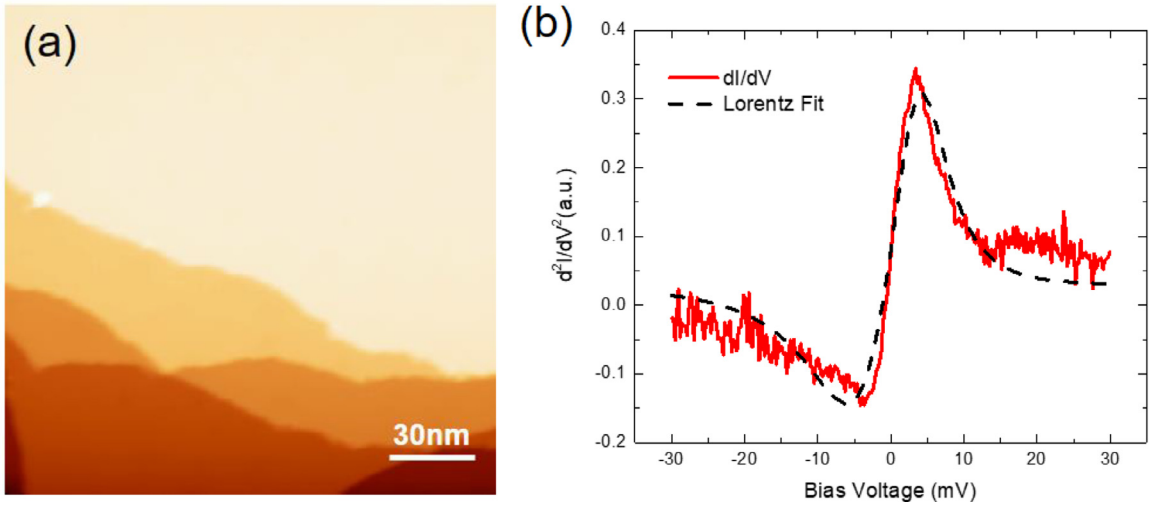

Fig. 1. (a) STM topographic image of clean Cu(100) surface taken at 5 K in constant current mode with tunneling current of 10 pA and sample bias of 2 V. (b) A representative STM-IETS spectrum obtained on clean Cu(100) surface with modulation voltage of 3.0 mV. Spectrum is fitted by two Lorentz curves centered at ± 3.6 mV.

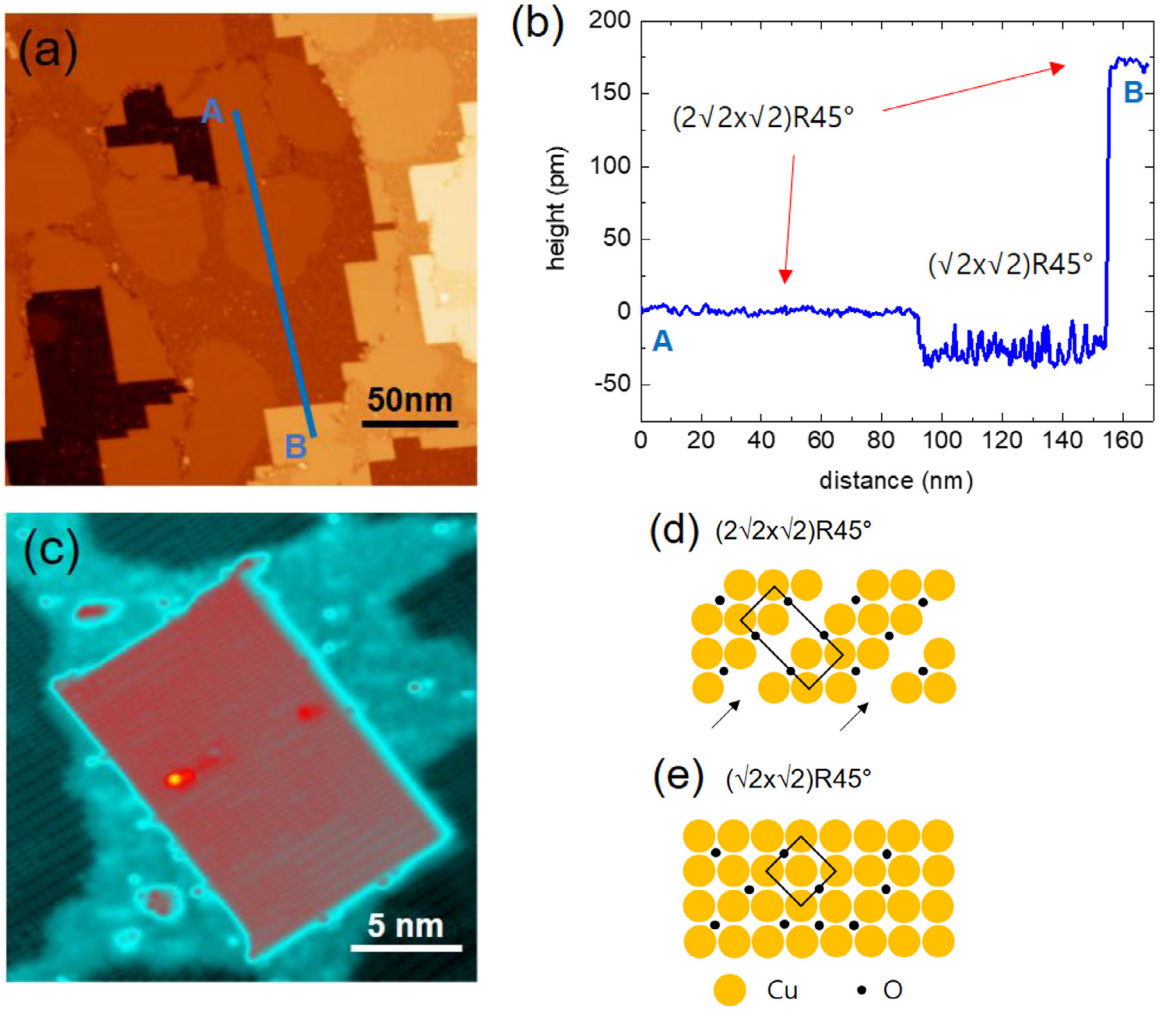

Fig. 2. (a) STM topographic image of the copper-oxide surface obtained with a tunneling current of 50 pA and sample bias of 2 V. (b) Height profile taken along the blue line in (a). (c) High-resolution image of the copper-oxide surface obtained with a tunneling current of 100 pA and sample bias of −50 mV. Cu-missing rows in the (2√2 × √2)R45°-O region are clearly visible, as explained in the main text. (d) Schematic of atomic arrangement on the (2√2 × √2)R45°-O surface. The black rectangle shows a unit cell of (2√2 × √2)R45°-O, and black arrows indicate Cu-missing rows. (e) Schematic of atomic arrangement on the (√2 × √2)R45°-O surface. The black rectangle shows a unit cell of the (√2 × √2)R45°-O surface, and oxygen atoms occupy the center hollow sites. (For interpretation of the references to color in this figure legend, the reader is referred to the web version of this article.)

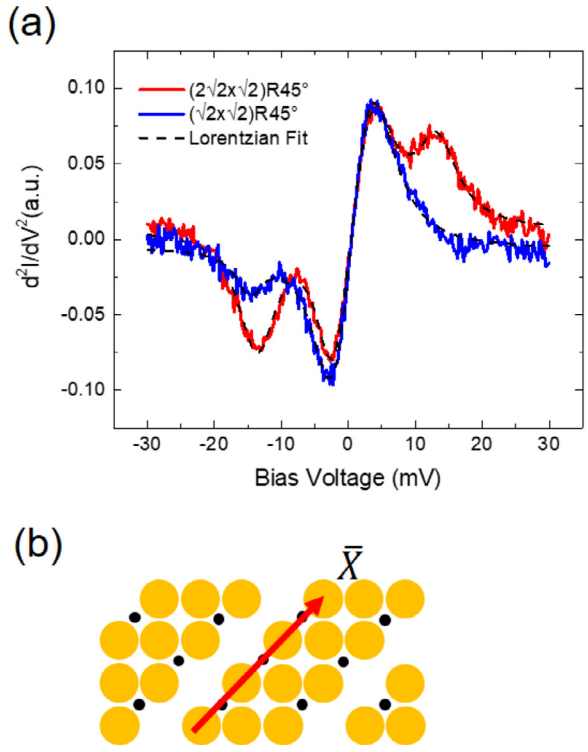

Fig. 3. (a) STM-IETS spectra obtained on (2√2 × √2)R45°-O surface (red) and (√2 × √2)R45°-O surface (blue) with a modulation voltage of 3.0 mV. (b) Schematics for enhanced phonon mode with *X* direction after creating Cu-missing rows. (For interpretation of the references to color in this figure legend, the reader is referred to the web version of this article.)

and STM-IETS spectra were acquired at the clean surface as a reference to observe the change in phonon mode peaks after oxygen exposure. All STM measurements in this study were performed at ~5 K. The STM-IETS signal, d^2I/dV^2 signal, was measured by the lockin technique with the modulation voltage of 3.0 mV and at the frequency of 211 Hz. Fig. 1(b) shows a representative STM-IETS spectrum that reveals a phonon mode on the clean Cu(100) surface at 3.6 meV with the full width half maximum (FWHM) of 10.6 meV, which were extracted by Lorentzian fitting. This peak width is similar to those in earlier STM-IETS studies on metal surfaces [15,18]. The observation of this peak is debated because no VHS exists at this energy in the phonon density of states. Vitali et al. [18] suggested that this peak could have originated from the atomic vibration at the tip apex. However, Minamitani et al. [15] proposed that the out-of-plane polarized surface acoustic phonon near the Γ point in STM-IETS. In our experiment, this peak width was reproduced in the measurements with different STM tips and samples. We believe that this peak arises from the acoustic phonon mode near the Γ point and not from the atomic vibration at the tip apex.

After measuring clean Cu(100), the surface was exposed to oxygen to induce surface relaxation on the surface. To grow the ordered oxygen-adsorbed layer, a clean Cu surface was heated to 450 °C at 1×10^{-10} Torr followed by exposure to oxygen at ~3000 Langmuir at 200 °C [19–21]. Fig. 2(a) shows an STM topographic image of the oxygen-adsorbed Cu(100) surface, in which two different surface reconstruction regions coexist. One region appears flat and the other appears rough. The line profile across these two regions clearly shows different roughness values of ~6 pm and 25 pm, respectively, as shown in Fig. 2(b). Based on previous studies [19,20] and the magnified STM image (Fig. 2(c)), the atomic structure of the flat region is revealed to have (2√2 × √2)R45°-O surface reconstruction and that of the rough region is revealed to have a disordered (1 × 1) structure, locally (√2 × √2)R45°-O surface reconstruction. In the (2√2 × √2)R45°-O surface, oxygen atoms are located at the center hollow sites of the Cu lattice with consecutive missing Cu rows, as shown in Fig. 2(d). The missing rows are clearly visible at the center rectangular region of the magnified STM image (Fig. 2(c)), as indicated by black arrows in Fig. 2(d). In the disordered (√2 × √2)R45°-O surface, oxygen atoms are located at the same sites as in the (2√2 × √2)R45°-O surface; however, no rows with missing Cu exist, as shown in Fig. 2(e).

To study the effect of oxygen atoms on surface phonon modes, STM-IETS spectra obtained on the (2√2 × √2)R45°-O and (√2 × √2)R45°-O surfaces were compared with those obtained on the clean Cu(100) surface, as shown in Fig. 3(a). These IETS spectra have two phonon modes at 3.5 meV and 13.5 meV with a FWHM of 7.0 meV extracted by Lorentzian fitting. The lower-energy mode is measured nearly at the same energy on the clean surface, implying that oxygen atoms affect little on the out-of-plane polarized surface phonon mode near the Γ point (3.5 meV versus 3.6 meV). Second, the out-of-plane surface mode at 13.5 meV on the (2√2 × √2)R45°-O surface, which was previously resolved by EELS measurement [22], was measured for the first time using STM-IETS. This peak was hardly resolved on the disordered (√2 × √2)R45°-O surface and clean Cu(100) surface. The resolution of this peak can be explained by the surface symmetry from Cu-missing rows on the (2√2 × √2)R45°-O surface. This peak is related to the out-of-plane surface mode peak at the *X* point of the Brillion zone boundary in the phonon dispersion relation [23], which is, owing to symmetry, parallel to the direction of the Cu-missing rows in real space, as shown in Fig. 3(b). Therefore, on the (2√2 × √2)R45°-O surface with Cu-missing rows, this phonon peak can be enhanced selectively. However, on the disordered (√2 × √2)R45°-O surface without Cu-missing rows, the signal of this phonon peak is not enhanced, which is similar to the STM-IETS on clean Cu(100) (see Fig. 1(b)). In addition, since oxygen-adsorbates impart compressive stress on the Cu(100) surface [24], the surface phonon mode of oxygen-adsorbed Cu(100) will have a smaller value than that of clean Cu(100). However, the difference was so small that we could not find much difference.

To investigate local variations in phonon modes, d^2I/dV^2 map was obtained over a coexisting area between two oxidized surfaces. Fig. 4(a) and (b) shows an STM topographic image and a d^2I/dV^2 map of the same area focused at a bias voltage of −15.0 mV. The topographic image shows the (2√2 × √2)R45°-O phase at the center and the disordered (√2 × √2)R45°-O phase on the right (same layer as the center phase) and left (one Cu layer lower than the center phase). As shown in Fig. 4(b), the average intensity of d^2I/dV^2 in the (2√2 × √2)R45°-O phase is larger than that in the disordered (√2 × √2)R45°-O phase. It is clearly visible in the height of the dotted lines in the cross-sectional profile in Fig. 4(c). In addition to the height difference in two phases, there strong local variation of d^2I/dV^2 signal with the width of approximately 1 nm, appeared bright lines from the bottom left to top right in the Fig. 4(b) and sharp peaks in the cross-sectional profile in Fig. 4(c). It is noted that this d^2I/dV^2 map was obtained at the bias voltage of −15.0 mV. There are two possible scenarios. This lines reflect the local surface stress at oxygen-adsorbed surfaces [24], resulting in enhanced d^2I/dV^2 signal. A similar stress relaxation was observed on the double Fe layer on the W(100) surface [25,26]. The second possibility is the electronic structural change in the region at the stressed regions. That is because the intensity of d^2I/dV^2 is proportional to the product of the electron–phonon coupling matrix elements and the phonon density of states [15]. Therefore, we cannot determine whether these peaks are originated from the change of the local electronic structure or the phononic structure with STM-IETS measurements.

In conclusion, surface phonon modes on clean and oxygen-adsorbed Cu(100) surfaces were successfully resolved using the STM-IETS technique. The acoustic phonon modes were successfully resolved and they are modified under the stress caused by oxygen adsorption. The directionality of the phonon mode, in combination with the surface symmetry, is directly related to the STM-IETS signal strength.

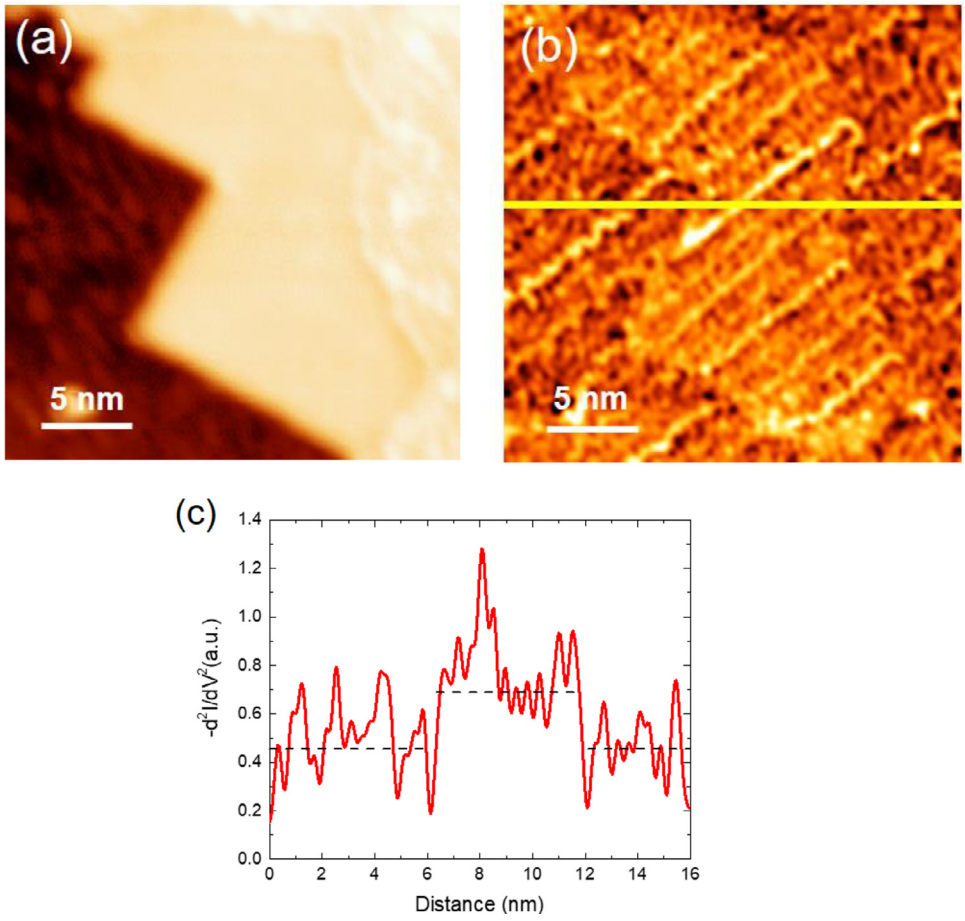

Fig. 4. (a) STM topographic image of a copper-oxide surface obtained with a tunneling current of 100 pA and sample bias of 500 mV. (b) STM-IETS map of the same area as in (a) with a tunneling current of 100 pA and bias voltage of −15 mV. All scale bars indicate 5 nm. (c) Height profile across the yellow line in (b). (For interpretation of the references to color in this figure legend, the reader is referred to the web version of this article.)

Acknowledgments

This work is supported in part by the National Research Foundation of Korea (NRF) Grant (NRF-2006-0093847 and NRF-2010-00349). JSC was supported by the IBS research program IBS-R027-D1.

References

[1] M.H. Mohamed, L.L. Kesmodel, B.M. Hall, D.L. Mills, Surface phonon dispersion on Cu(111), Phys. Rev. B 37 (1988) 2763.
[2] U. Harten, J.P. Toennies, C. Wöll, G. Zhang, Observation of a Kohn anomaly in the surface-phonon dispersion curves of Pt(111), Phys. Rev. Lett. 55 (1985) 2308.
[3] J. Kröger, Electron–phonon coupling at metal surfaces, Rep. Prog. Phys. 69 (2006) 899.
[4] B.C. Stipe, M.A. Rezaei, W. Ho, Single-molecule vibrational spectroscopy and microscopy, Science 280 (1998) 1732.
[5] C. Chiang, C. Xu, Z. Han, W. Ho, Real-space imaging of molecular structure and chemical bonding by single-molecule inelastic tunneling probe, Science 344 (2014) 885.
[6] L.J. Lauhon, W. Ho, Single-molecule chemistry and vibrational spectroscopy: Pyridine and benzene on Cu(001), J. Phys. Chem. A 104 (2000) 2463.
[7] L.J. Lauhon, W. Ho, Single-molecule vibrational spectroscopy and microscopy: CO on Cu(001) and Cu(110), Phys. Rev. B 60 (1999) R8525.
[8] A.J. Heinrich, J.A. Gupta, C.P. Lutz, D.M. Eigler, Single-atom spin-flip spectroscopy, Science 306 (2004) 466.
[9] C.F. Hirjibehedin, C.P. Lutz, A.J. Heinrich, Spin coupling in engineered atomic structures, Science 312 (2006) 1021.
[10] J.C. Oberg, M.R. Calvo, F. Delgado, M. Moro-Lagares, D. Serrate, D. Jacob, J. Fernández-Rossier, C.F. Hirjibehedin, Control of single-spin magnetic anisotropy by exchange coupling, Nat. Nanotechnol. 9 (2014) 64.
[11] C.F. Hirjibehedin, C.-Y. Lin, A.F. Otte, M. Ternes, C.P. Lutz, B.A. Jones, A.J. Heinrich, Large magnetic anisotropy of a single atomic spin embedded in a surface molecular network, Science 317 (2007) 1199.
[12] L. Vitali, M.A. Schneider, K. Kern, L. Wirtz, A. Rubio, Phonon and plasmon excitation in inelastic electron tunneling spectroscopy of graphite, Phys. Rev. B 69 (2004) 121414.
[13] F.D. Natterer, Y. Zhao, J. Wyrick, Y.-H. Chan, W.-Y. Ruan, M.-Y. Chou, K. Watanabe, T. Taniguchi, N.B. Zhitenev, J.A. Stroscio, Strong asymmetric charge carrier dependence in inelastic electron tunneling spectroscopy of graphene phonons, Phys. Rev. Lett. 114 (2015) 245502.
[14] H. Gawronski, M. Mehlhorn, K. Morgenstern, Imaging phonon excitation with atomic resolution, Science 319 (2008) 930.
[15] E. Minamitani, R. Arafune, N. Tsukahara, Y. Ohda, S. Watanabe, M. Kawai, H. Ueba, N. Takagi, Surface phonon excitation on clean metal surfaces in scanning tunneling microscopy, Phys. Rev. B 93 (2016) 085411.
[16] N. Okabayashi, A. Gustafsson, A. Peronio, M. Paulsson, T. Arai, F.J. Giessibl, Influence of atomic tip structure on the intensity of inelastic tunneling spectroscopy data analyzed by combined scanning tunneling spectroscopy, force microscopy, and density functional theory, Phys. Rev. B 93 (2016) 165415.
[17] B.N.J. Persson, A. Baratoff, Inelastic electron tunneling from a metal tip: The contribution from resonant processes, Phys. Rev. Lett. 59 (1987) 339.
[18] L. Vitali, S.D. Borisova, G.G. Rusina, E.V. Chulkov, K. Kern, Inelastic electron tunneling spectroscopy: A route to the identification of the tip-apex structure, Phys. Rev. B 81 (2010) 153409.
[19] T. Fujita, Y. Okawa, Y. Matsumoto, K. Tanaka, Phase boundaries of nanometer scale c(2×2)-O domains on the Cu(100) surface, Phys. Rev. B 54 (1996) 2167.
[20] K. Lahtonen, M. Hirsimäki, M. Lampimäki, M. Valden, Oxygen adsorption-induced nanostructures and island formation on Cu{100}: Bridging the gap between the formation of surface confined oxygen chemisorption layer and oxide formation, J. Chem. Phys. 129 (2008) 124703.
[21] M. Lampimäki, K. Lahtonen, M. Hirsimäki, M. Valden, Nanoscale oxidation of Cu (100): Oxide morphology and surface reactivity, J. Chem. Phys. 126 (2007) 034703.
[22] M. Wuttig, R. Franchy, H. Ibach, Oxygen on Cu(100) – a case of an adsorbate induced reconstruction, Surf. Sci. 213 (1989) 103.
[23] M. Alcántara Ortigoza, R. Heid, K.-P. Bohnen, T.S. Rahman, Effect of c(2×2)-CO overlayer on the phonons of Cu(001): A first-principles study, Phys. Rev. B 79 (2009) 125432.
[24] M.J. Harrison, D.P. Woodruff, J. Robinson, D. Sander, W. Pan, J. Kirschner, Adsorbate-induced surface reconstruction and surface-stress changes in Cu(100)/O: Experiment and theory, Phys. Rev. B 74 (2006) 165402.
[25] A. Schlenhoff, S. Krause, G. Herzog, R. Wiesendanger, Bulk Cr tips with full spatial magnetic sensitivity for spin-polarized scanning tunneling microscopy, Appl. Phys. Lett. 97 (2010) 083104.
[26] H. Bethge, D. Heuer, C. Jensen, K. Reshöft, U. Köhler, Misfit-related effects in the epitaxial growth of iron on W(110), Surf. Sci. 331–333 (1995) 878.